XXII. International Workshop on Deep-Inelastic Scattering
April 28 – May 2, Warsaw

Dihadron production at Jefferson Lab.

Sergio Anefalos Pereira
(INFN - Frascati)

Istituto Nazionale di Fisica Nucleare

CEBAF Large Acceptance Spectrometer

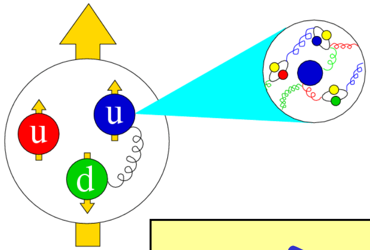

Physics Motivation

Describe complex nucleon structure in terms of partonic degrees of freedom of QCD

- in the collinear approximation there are 3 leading twist PDFs + 3 twist-3 PDFs which survive the integration over the transverse momentum. They give a detailed picture of the nucleon in longitudinal momentum space;
- the goal of the present work is to extract the two twist-3 collinear distribution functions *e(x) and* $h_L(x)$ looking at dihadron SIDIS, where:

N \ q	U	L	T
U	number density f_1		e
L		helicity g_1	h_L
T		g_T	transversity h_1

e(x) : sub-leading twist PDF of transverse polarized quark in an unpolarized nucleon

$h_L(x)$: sub-leading twist PDF of transverse polarized quark in a longitudinally polarized nucleon

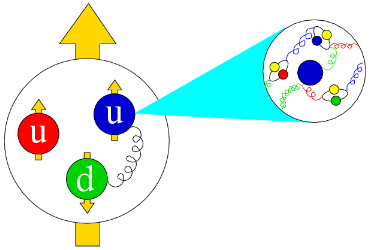

Physics Motivation

PRD 67, 114014 (2003)

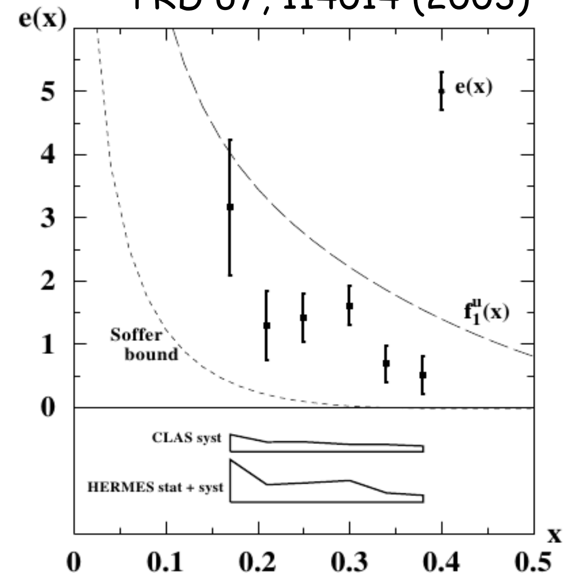

The twist-3 PDFs *e(x)* and $h_L(x)$ contains important information on the quark-gluon correlations. The first extraction of *e(x)* [PRD 67, 114014 (2003)] has been done using single-pion CLAS data [PRD 69, 112004 (2004)]

There are also some model predictions:

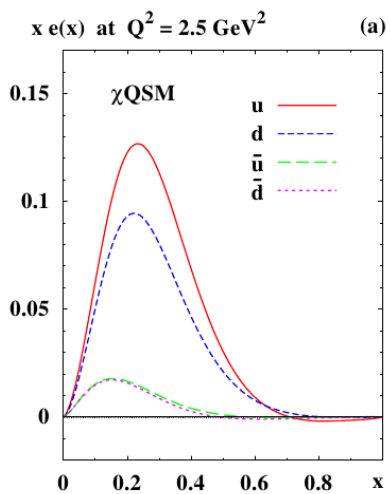

chiral quark soliton (χQSM)
Phys. Rev. D64 (2001) 034013

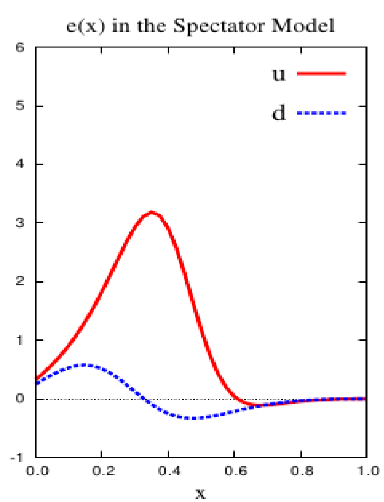

spectator model
Nucl. Phys. A626 (1997) 937

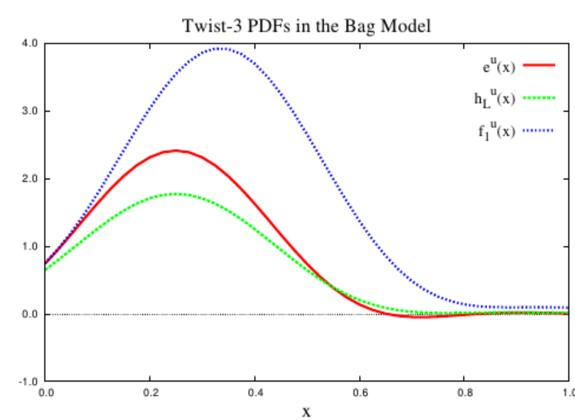

bag model
Nucl. Phys. B375 (1992) 527

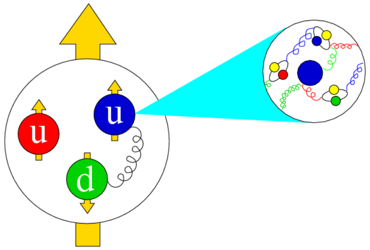

Physics Motivation

On the other hand, $h_L(x)$ has only some model predictions

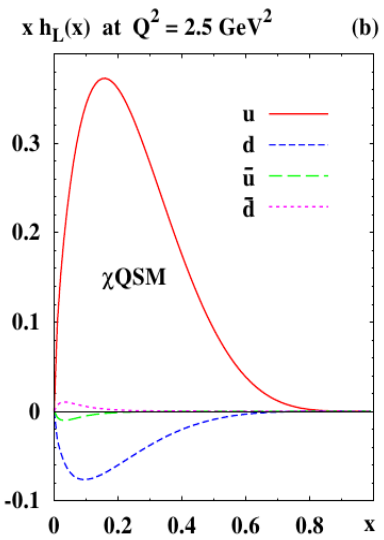

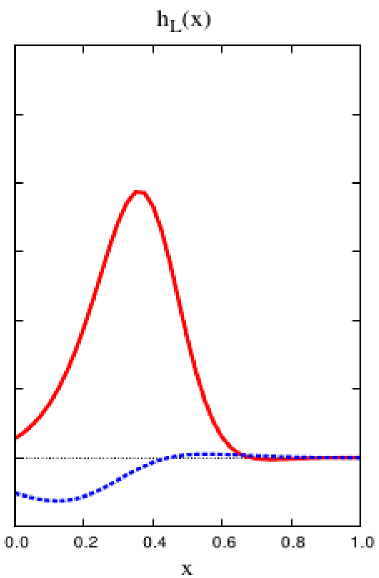

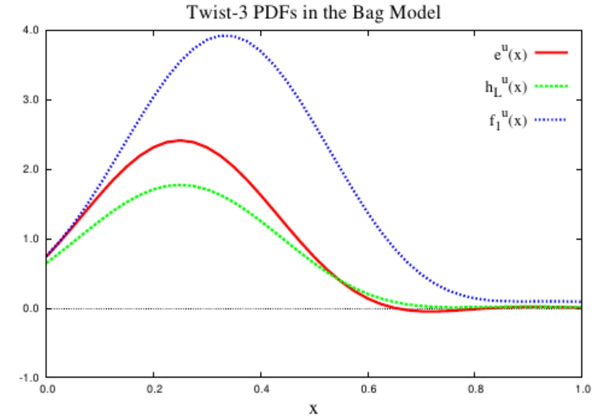

chiral quark soliton (χQSM)
Phys. Rev. D64 (2001) 034013

spectator model
Nucl. Phys. A626 (1997) 937

bag model
Nucl. Phys. B375 (1992) 527

JLab Accelerator CEBAF

- Continuous Electron Beam
- Energy up to 6 GeV
- 1nA - 200μA simultaneous beam in different halls
- polarization up to 85%

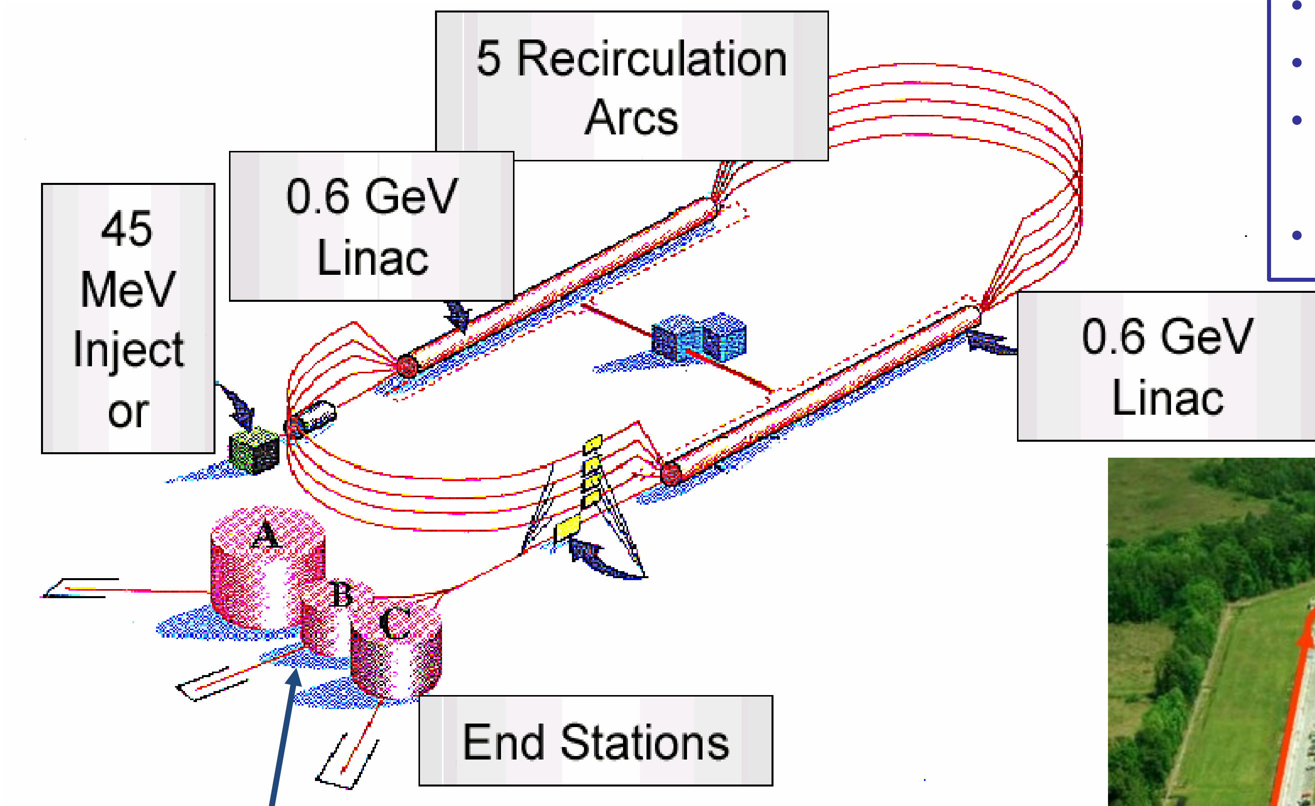

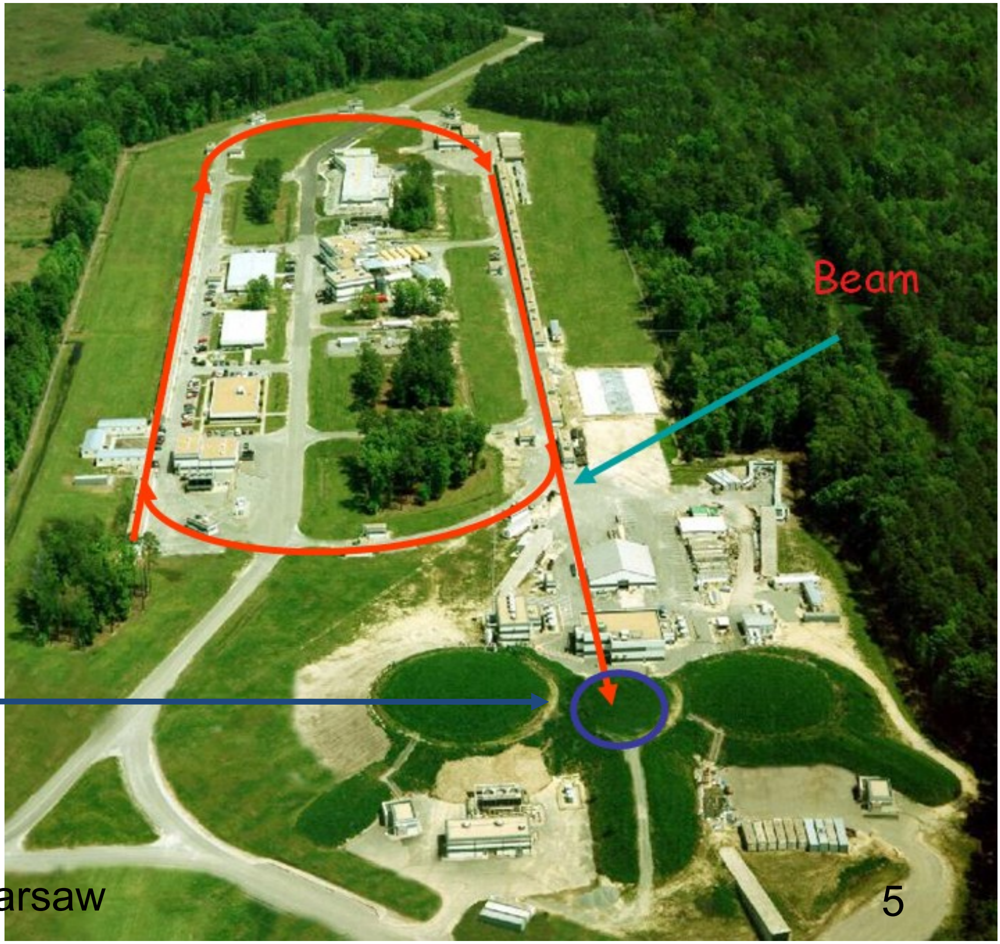

CLAS

Hall B: Cebaf Large Acceptance Spectrometer (CLAS)

Torus magnet
6 superconducting coils

Liquid D_2 (H_2)target +
γ start counter; e minitorus

Drift chambers
argon/CO_2 gas, 35,000 cells

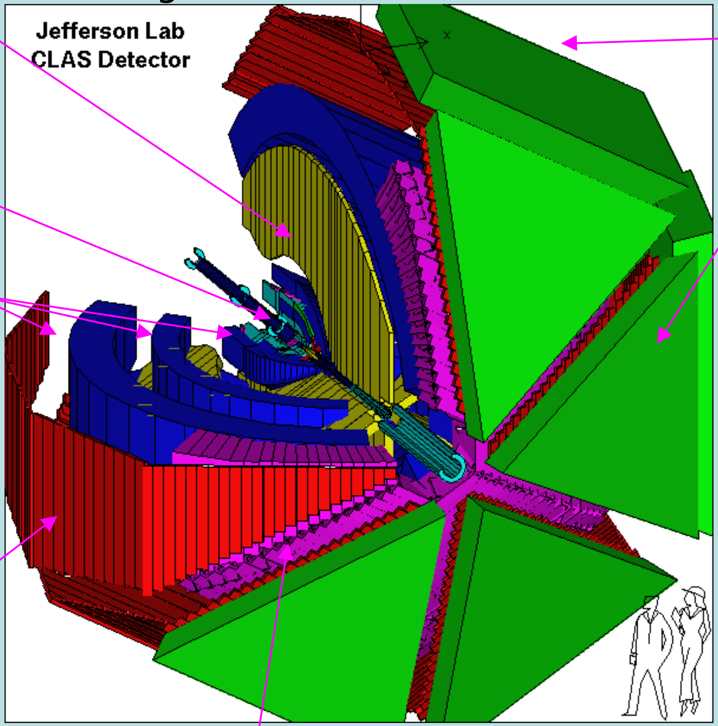

Electromagnetic calorimeters
Lead/scintillator, 1296 photomultipliers

- Broad angular coverage (8° - 140° in LAB frame)
- Charged particle momentum resolution ~0.5% forward direction

CLAS is designed to measure exclusive reactions with multi-particle final states

Time-of-flight counters
plastic scintillators, 684 photomultipliers

Gas Cherenkov counters
e/π separation, 216 PMTs

The eg1-dvcs experiment

- beam polarization ~ 85%
- proton polarization ~ 80%
- used the Inner Calorimeter (in addition to the EC) to detect photons at small angles.

Part A

Hydrogen target (NH_3)
Beam energy: 5.892 GeV
4.735 GeV
Luminosity: 22.7 fb^{-1}

Part B

Hydrogen target (NH_3)
Beam energy: 5.967 GeV
Luminosity: 50.7 fb^{-1}

Part C

Deuterium target (ND_3)
Beam energy: 5.764 GeV
Luminosity: 25.3 fb^{-1}

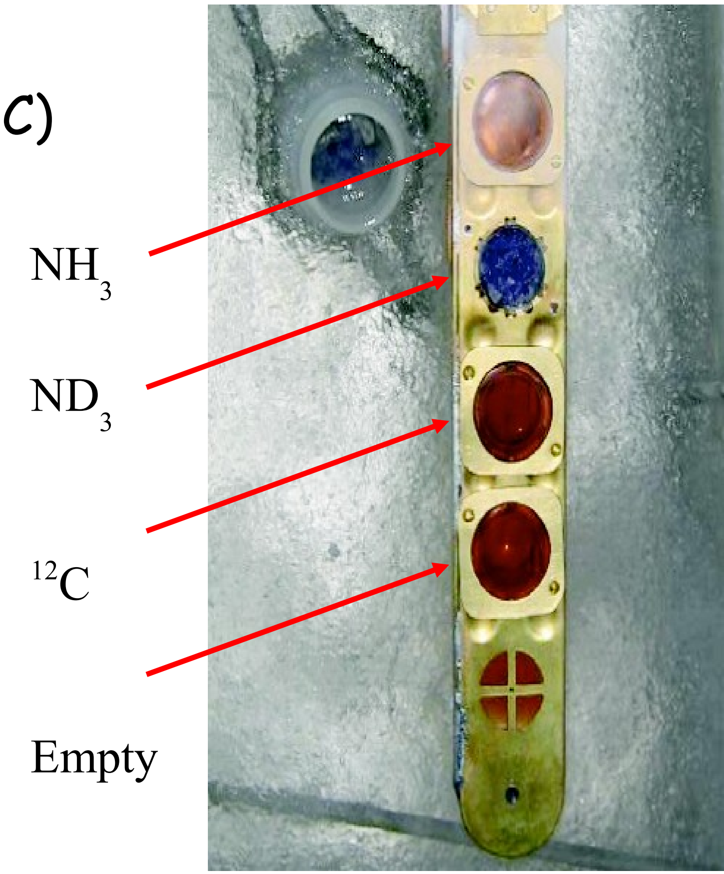

Runs with ^{12}C target for background evaluation

SIDIS observables and kinematical planes

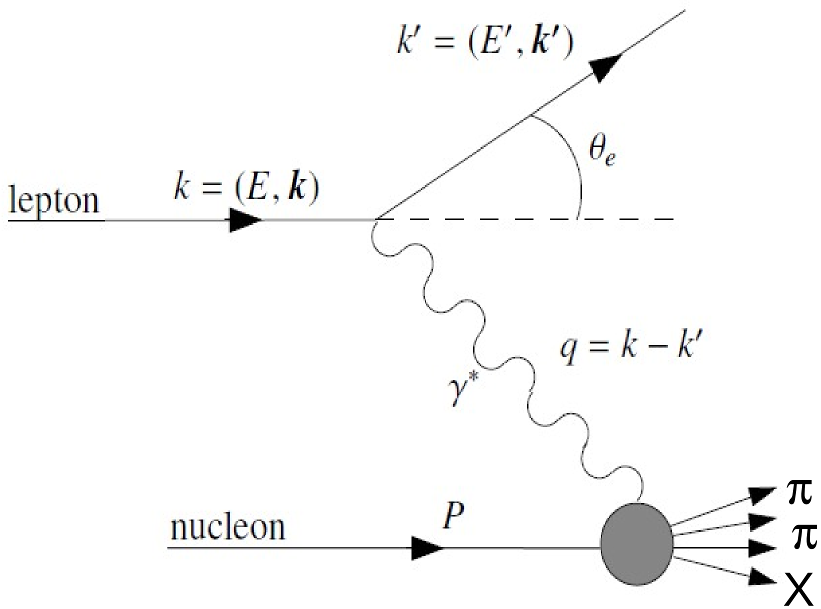

$$\nu = E - E'$$

$$Q^2 = (k - k')^2$$

$$y = \nu / E$$

$$x = Q^2 / 2M\nu$$

$$z = E_h / \nu$$

the fraction of the virtual-photon energy carried by the two hadrons

$$x_F = \frac{2\, p_{\parallel}}{W}$$

longitudinal momentum fraction carried by the hadron, where *W* is the γ*-p center-of-mass energy

Definition of azimuthal and polar angles

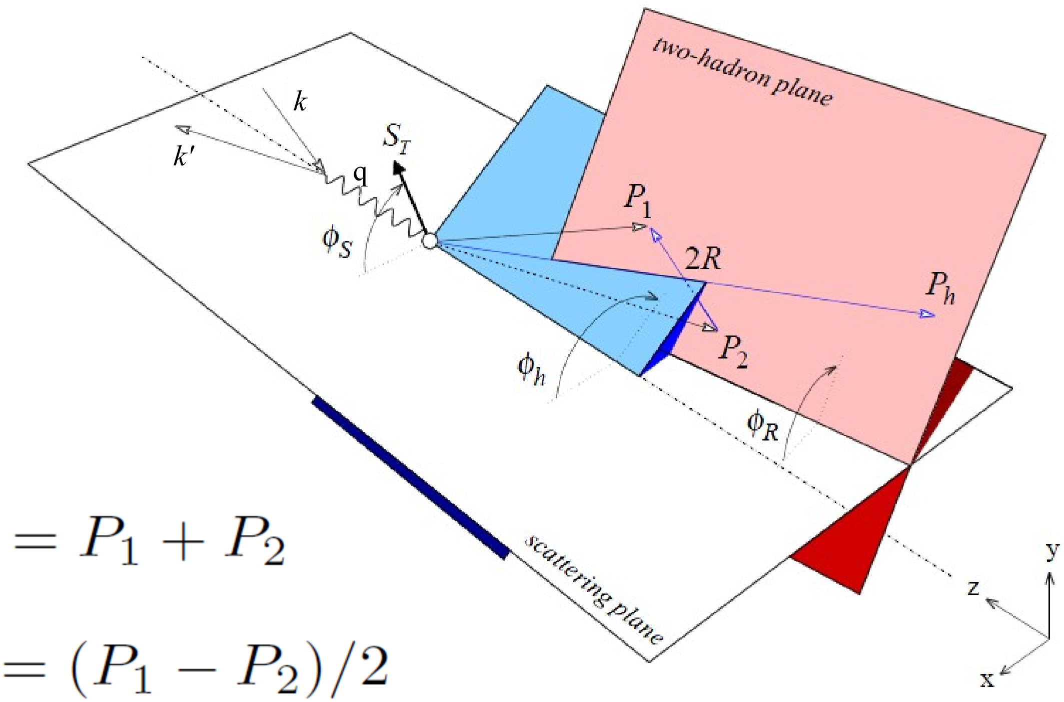

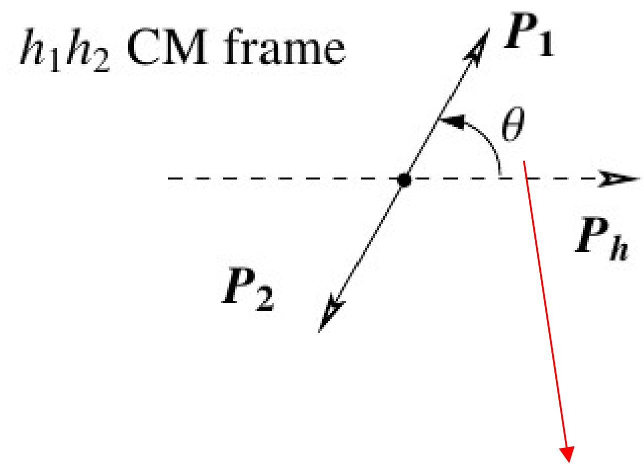

$$P_h = P_1 + P_2$$

$$R = (P_1 - P_2)/2$$

$$\phi_R = \frac{\boldsymbol{q} \times \boldsymbol{k} \cdot \boldsymbol{R}_T}{|\boldsymbol{q} \times \boldsymbol{k} \cdot \boldsymbol{R}_T|} \cos^{-1} \frac{\boldsymbol{q} \times \boldsymbol{k} \cdot \boldsymbol{q} \times \boldsymbol{R}_T}{|\boldsymbol{q} \times \boldsymbol{k}||\boldsymbol{q} \times \boldsymbol{R}_T|}$$

the angle between the direction of P_1 in the $\pi^+ \pi^-$ center-of-mass frame, and the direction of P_h in the photon-target rest frame.

Structure functions in terms of PDF and DiFF

$$F_{UU,T} = x\, f_1^q(x)\, D_1^q(z, \cos\theta, M_h)$$

$$F_{UU,L} = 0$$

$$F_{UU}^{\cos\phi_R} = -x \frac{|R|\sin\theta}{Q} \frac{1}{z} f_1^q(x)\, \tilde{D}^{\sphericalangle q}(z, \cos\theta, M_h)$$

$$F_{UU}^{\cos 2\phi_R} = 0$$

$$F_{LU}^{\sin\phi_R} = -x \frac{|R|\sin\theta}{Q} [\frac{M}{M_h} x\, e^q(x)\, H_1^{\sphericalangle q}(z, \cos\theta, M_h) + \frac{1}{z} f_1^q(x)\, \tilde{G}^{\sphericalangle q}(z, \cos\theta, M_h)]$$

$$F_{UL}^{\sin\phi_R} = -x \frac{|R|\sin\theta}{Q} [\frac{M}{M_h} x\, h_L^q(x)\, H_1^{\sphericalangle q}(z, \cos\theta, M_h) + \frac{1}{z} g_1^q(x)\, \tilde{G}^{\sphericalangle q}(z, \cos\theta, M_h)]$$

$$F_{UL}^{\sin 2\phi_R} = 0$$

$$F_{LL} = x\, g_1^q(x)\, D_1^q(z, \cos\theta, M_h)$$

$$F_{LL}^{\cos\phi_R} = -x \frac{|R|\sin\theta}{Q} \frac{1}{z} g_1^q(x)\, \tilde{D}_1^{\sphericalangle q}(z, \cos\theta, M_h)$$

Structure functions in terms of PDF and DiFF

$$F_{UU,T} = x\, f_1^q(x)\, D_1^q(z, \cos\theta, M_h)$$

$$F_{UU,L} = 0$$

$$F_{UU}^{\cos\phi_R} = -x \frac{|R|\sin\theta}{Q} \frac{1}{z} f_1^q(x)\, \tilde{D}^{\sphericalangle q}(z, \cos\theta, M_h)$$

$$F_{UU}^{cos2\phi_R} = 0$$

$$F_{LU}^{\sin\phi_R} = -x \frac{|R|\sin\theta}{Q} \left[\frac{M}{M_h} x\, e^q(x)\, H_1^{\sphericalangle q}(z, \cos\theta, M_h) + \frac{1}{z} f_1^q(x)\, \tilde{G}^{\sphericalangle q}(z, \cos\theta, M_h) \right]$$

$$F_{UL}^{\sin\phi_R} = -x \frac{|R|\sin\theta}{Q} \left[\frac{M}{M_h} x\, h_L^q(x)\, H_1^{\sphericalangle q}(z, \cos\theta, M_h) + \frac{1}{z} g_1^q(x)\, \tilde{G}^{\sphericalangle q}(z, \cos\theta, M_h) \right]$$

$$F_{UL}^{sin2\phi_R} = 0$$

$$F_{LL} = x\, g_1^q(x)\, D_1^q(z, \cos\theta, M_h)$$

$$F_{LL}^{\cos\phi_R} = -x \frac{|R|\sin\theta}{Q} \frac{1}{z} g_1^q(x)\, \tilde{D}_1^{\sphericalangle q}(z, \cos\theta, M_h)$$

Structure functions in terms of PDF and DiFF

$$F_{UU,T} = x f_1^q(x) D_1^q(z, \cos\theta, M_h)$$

$$F_{UU,L} = 0$$

$$F_{UU}^{\cos\phi_R} = -x \frac{|R|\sin\theta}{Q} \frac{1}{z} f_1^q(x) \tilde{D}^{\sphericalangle q}(z, \cos\theta, M_h)$$

$$F_{UU}^{\cos 2\phi_R} = 0$$

$$F_{LU}^{\sin\phi_R} = -x \frac{|R|\sin\theta}{Q} [\frac{M}{M_h} x e^q(x) H_1^{\sphericalangle q}(z, \cos\theta, M_h) + \frac{1}{z} f_1^q(x) \tilde{G}^{\sphericalangle q}(z, \cos\theta, M_h)]$$

$$F_{UL}^{\sin\phi_R} = -x \frac{|R|\sin\theta}{Q} [\frac{M}{M_h} x h_L^q(x) H_1^{\sphericalangle q}(z, \cos\theta, M_h) + \frac{1}{z} g_1^q(x) \tilde{G}^{\sphericalangle q}(z, \cos\theta, M_h)]$$

$$F_{UL}^{\sin 2\phi_R} = 0$$

$$F_{LL} = x g_1^q(x) D_1^q(z, \cos\theta, M_h)$$

$$F_{LL}^{\cos\phi_R} = -x \frac{|R|\sin\theta}{Q} \frac{1}{z} g_1^q(x) \tilde{D}_1^{\sphericalangle q}(z, \cos\theta, M_h)$$

Strategy behind the extraction of $e(x)$ and $h_L(x)$

$$F_{LU}^{\sin\phi_R} = -x\frac{|R|\sin\theta}{Q}\left[\frac{M}{M_h}x e^q(x) H_1^{\sphericalangle q}(z,\cos\theta,M_h) + \frac{1}{z} f_1^q(x)\tilde{G}^{\sphericalangle q}(z,\cos\theta,M_h)\right]$$ ~ 0

$$F_{UL}^{\sin\phi_R} = -x\frac{|R|\sin\theta}{Q}\left[\frac{M}{M_h}x h_L^q(x) H_1^{\sphericalangle q}(z,\cos\theta,M_h) + \frac{1}{z} g_1^q(x)\tilde{G}^{\sphericalangle q}(z,\cos\theta,M_h)\right]$$ ~ 0

in the Wandzura-Wilczek approx. for fragmentation functions
Phys. Lett. B72 (1977) 195

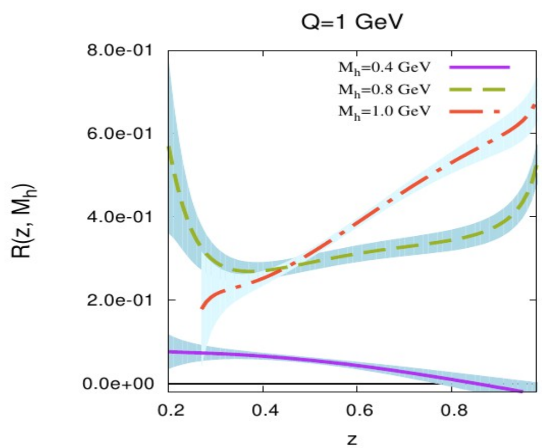

The $H_1^{\sphericalangle q}$ interference Fragmentation Function has been recently extracted by the Belle Collaboration from e^+/e^- data
PRD 85, 114023 (2012)

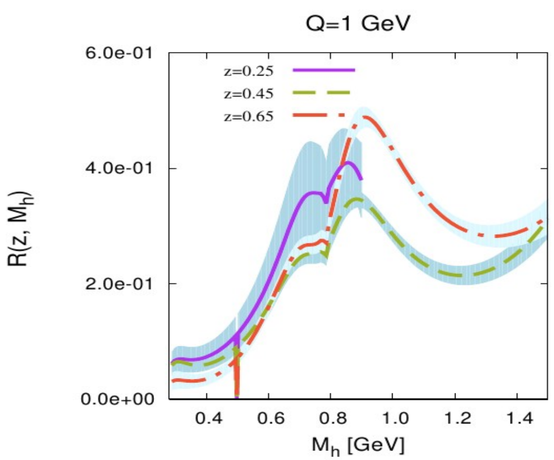

where $$R(z,M_h) = \frac{|R|}{M_h}\frac{H_1^{\sphericalangle u}(z,M_h;Q_0^2)}{D_1^u(z,M_h;Q_0^2)}$$

Analysis procedure

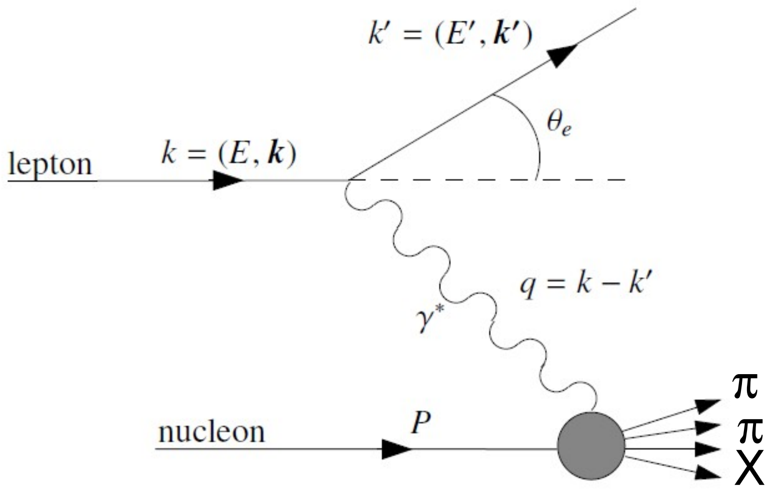

- ✓ semi-inclusive channel
- ✓ two topologies will be analyzed:
  - $e\,p \rightarrow e'\pi^+\pi^- X$
  - $e\,p \rightarrow e'\pi^+\pi^0 X \rightarrow e'\pi^+\gamma\gamma X$

- π^0 is identified as $M(\gamma\gamma)$

Current fragmentation region and SIDIS cut

$$x_F(\pi^{\pm}) > 0$$

the CFR comprise hadrons produced in the forward hemisphere (along the virtual photon)

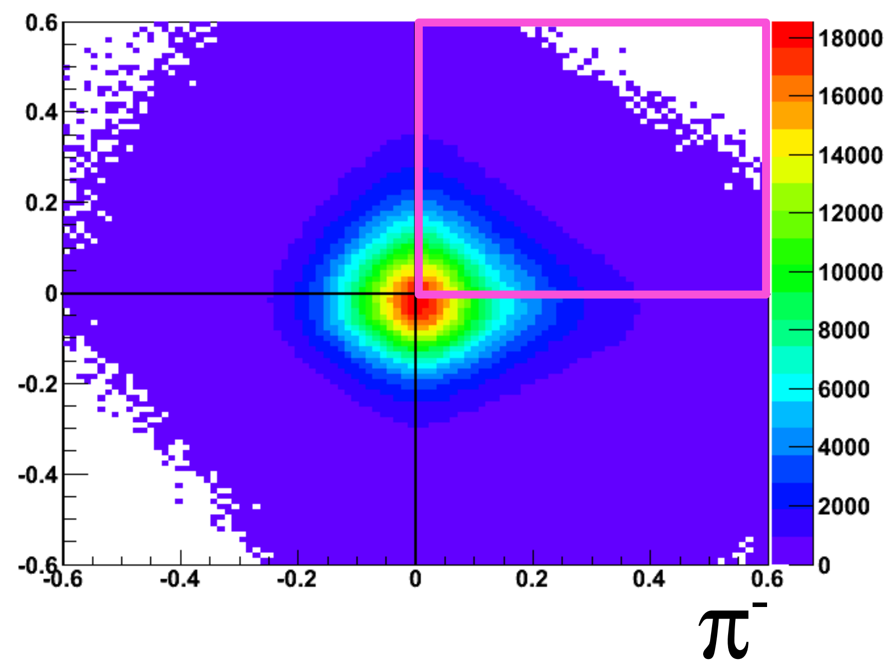

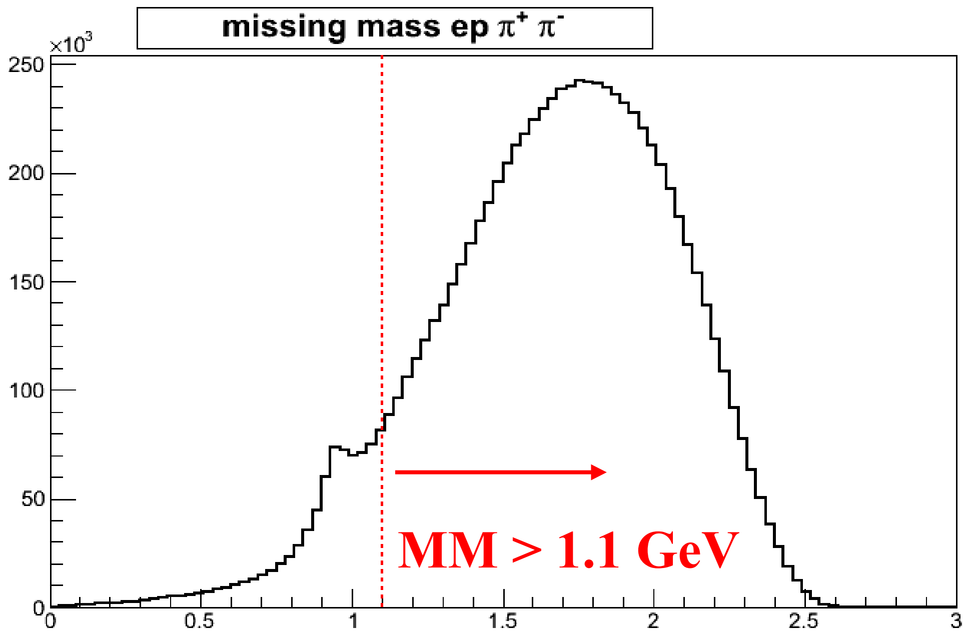

the final sample will be then binned in three variables: x, z, M_h

Beam-Spin Asymmetry (BSA)

$$A_{LU} = \frac{(N^{++} - N^{-+})P_t^- + (N^{+-} - N^{--})P_t^+}{P_B((N^{-+} + N^{++})P_t^- + (N^{--} + N^{+-})P_t^+)}$$

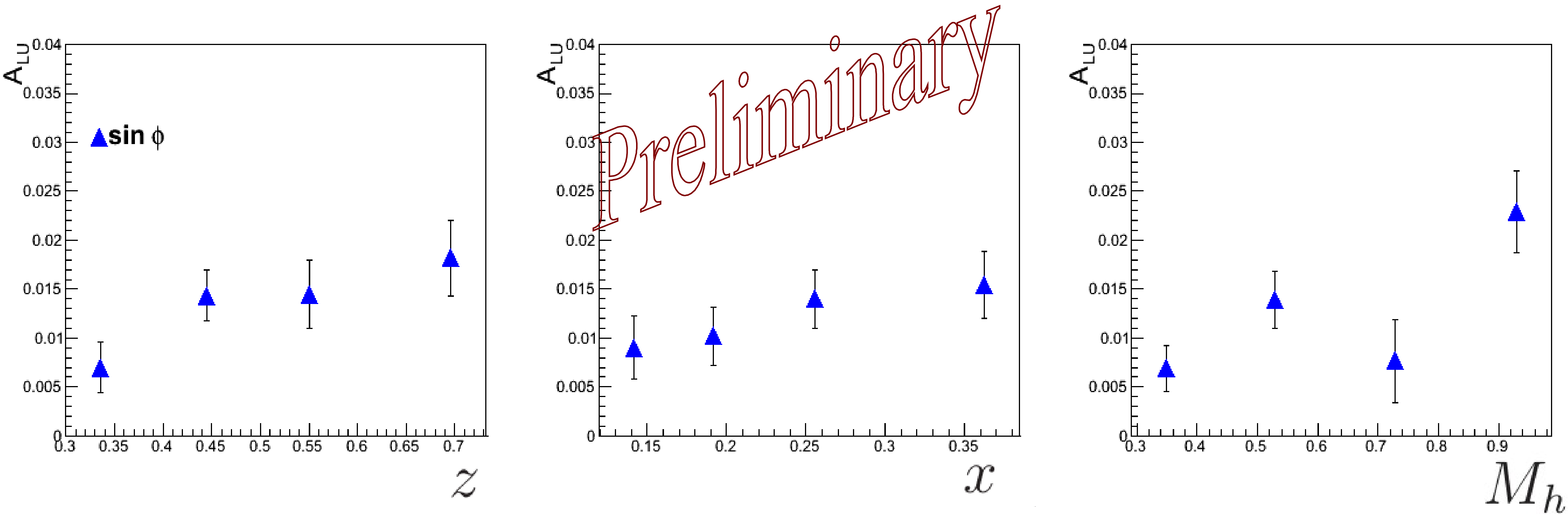

$$A_{LU} \propto e(x) H_1^{\sphericalangle q}(z, \cos\theta, M_h)$$

- *significantly non-zero asymmetries*
- *gives access to the sub-leading twist PDF e(x)*

Beam-Spin Asymmetry (BSA)

$$A_{LU} = \frac{\left(N^{++} - N^{-+}\right) P_t^{-} + \left(N^{+-} - N^{--}\right) P_t^{+}}{P_B\left(\left(N^{-+} + N^{++}\right) P_t^{-} + \left(N^{--} + N^{+-}\right) P_t^{+}\right)}$$

$$A_{LU} \propto e(x)\, H_1^{\sphericalangle q}(z, \cos\theta, M_h)$$

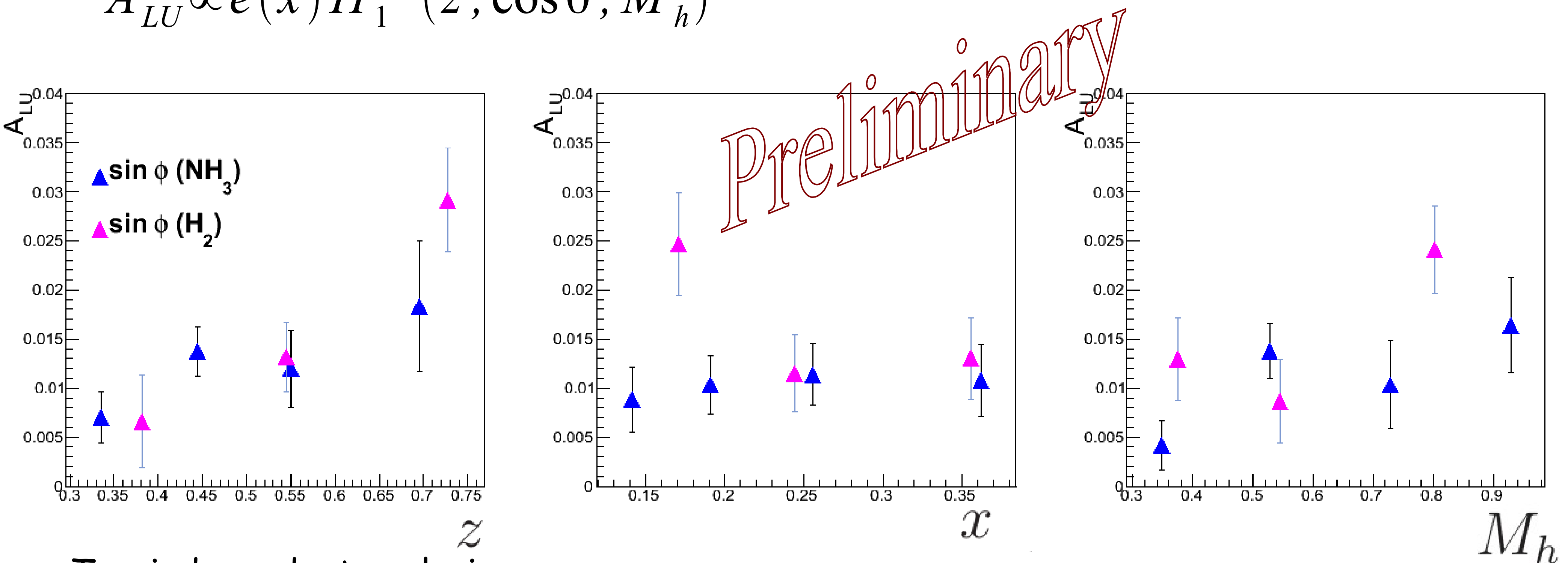

- Two independent analysis
- Two different experiments (unpolarized H_2 target (e1f) and longitudinally polarized NH_3 target (eg1-dvcs))
- Good agreement between the two analysis
- No nuclear effects observed

Target-Spin Asymmetry (TSA)

$$A_{UL} = \frac{1}{D_f} \frac{-N^{--} + N^{-+} - N^{+-} + N^{++}}{(N^{-+} + N^{++}) P_t^- + (N^{--} + N^{+-}) P_t^+}$$

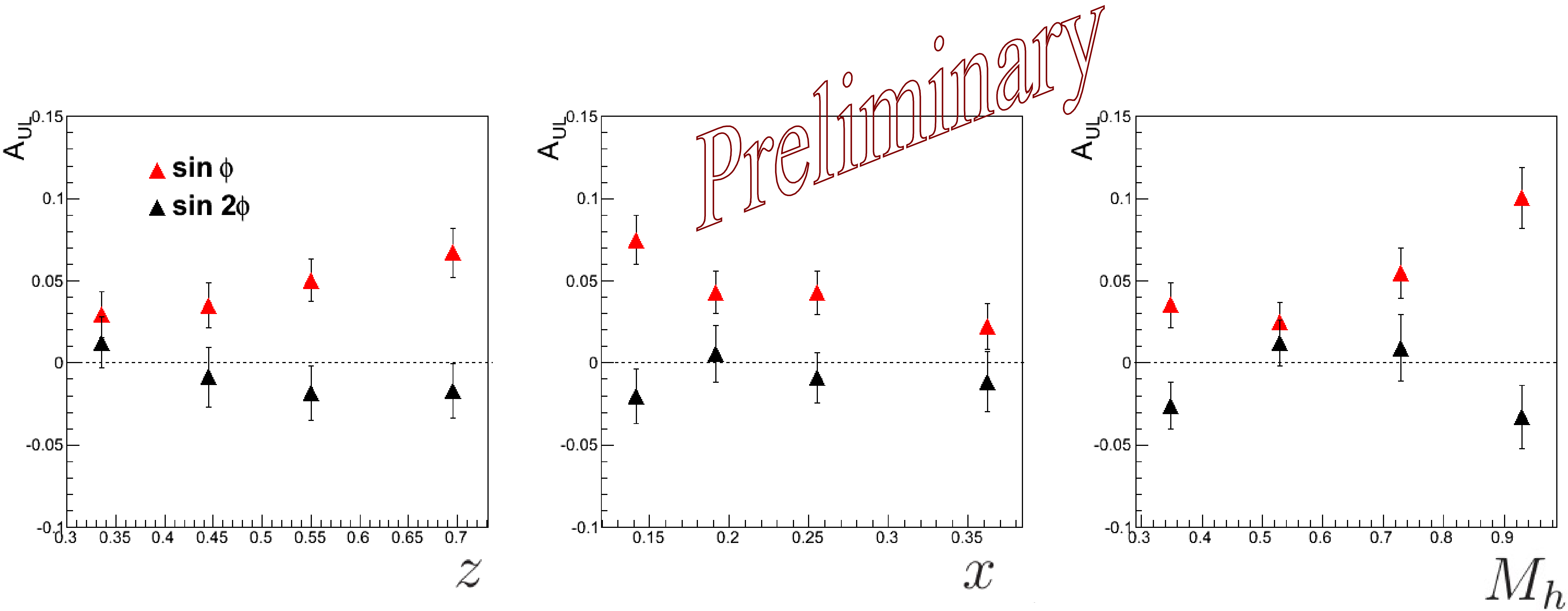

- significantly non-zero asymmetries
- DF = 0.18 has been used
- sin 2ϕ compatible with zero
- gives access to the sub-leading twist PDF $h_L(x)$

$$A_{UL} \propto h_L(x) H_1^{\sphericalangle q}(z, \cos\theta, M_h)$$

Beam- and Target-Spin Asymmetry comparison

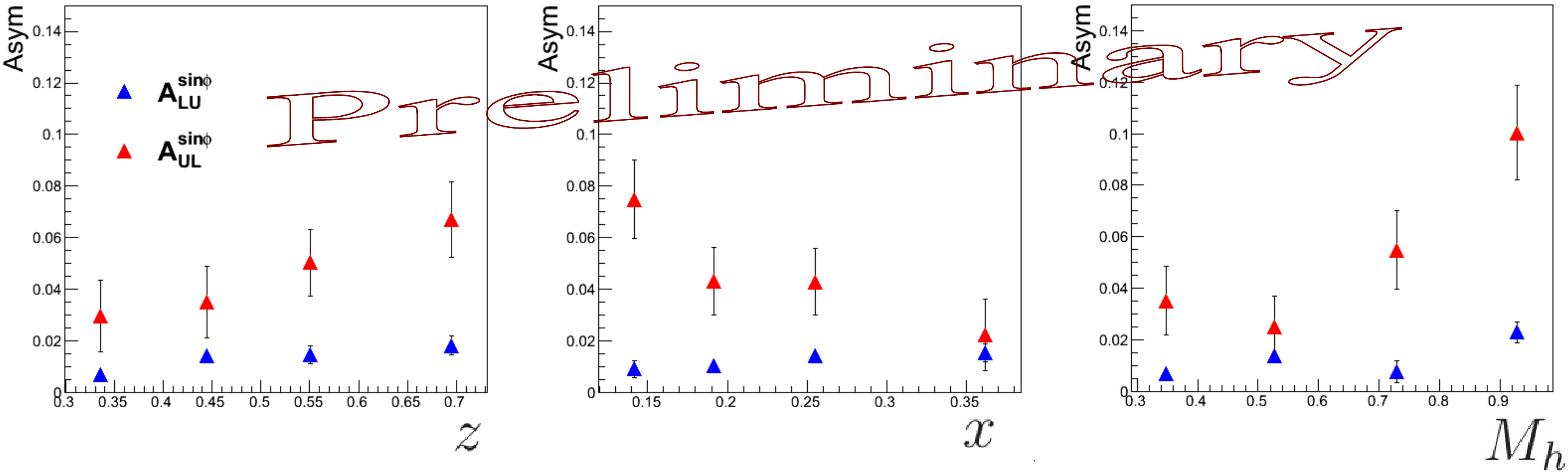

- Similar behavior for z and M_h dependence
- Opposite trend in the *x* dependence
- TSA higher than BSA, in some cases up to 5 times higher
- In the present approximation, the ratio A_{LU}/A_{UL} can provide information about the relative weights of *e(x)* and $h_L(x)$

$$\frac{A_{LU} \propto e(x) H_1^{\sphericalangle q}(z, \cos\theta, M_h)}{A_{UL} \propto h_L(x) H_1^{\sphericalangle q}(z, \cos\theta, M_h)}$$

Double-Spin Asymmetry (DSA)

$$A_{LL} = \frac{1}{D_f P_B} \frac{N^{--} - N^{-+} - N^{+-} + N^{++}}{(N^{-+} + N^{++}) P_t^- + (N^{--} + N^{+-}) P_t^+}$$

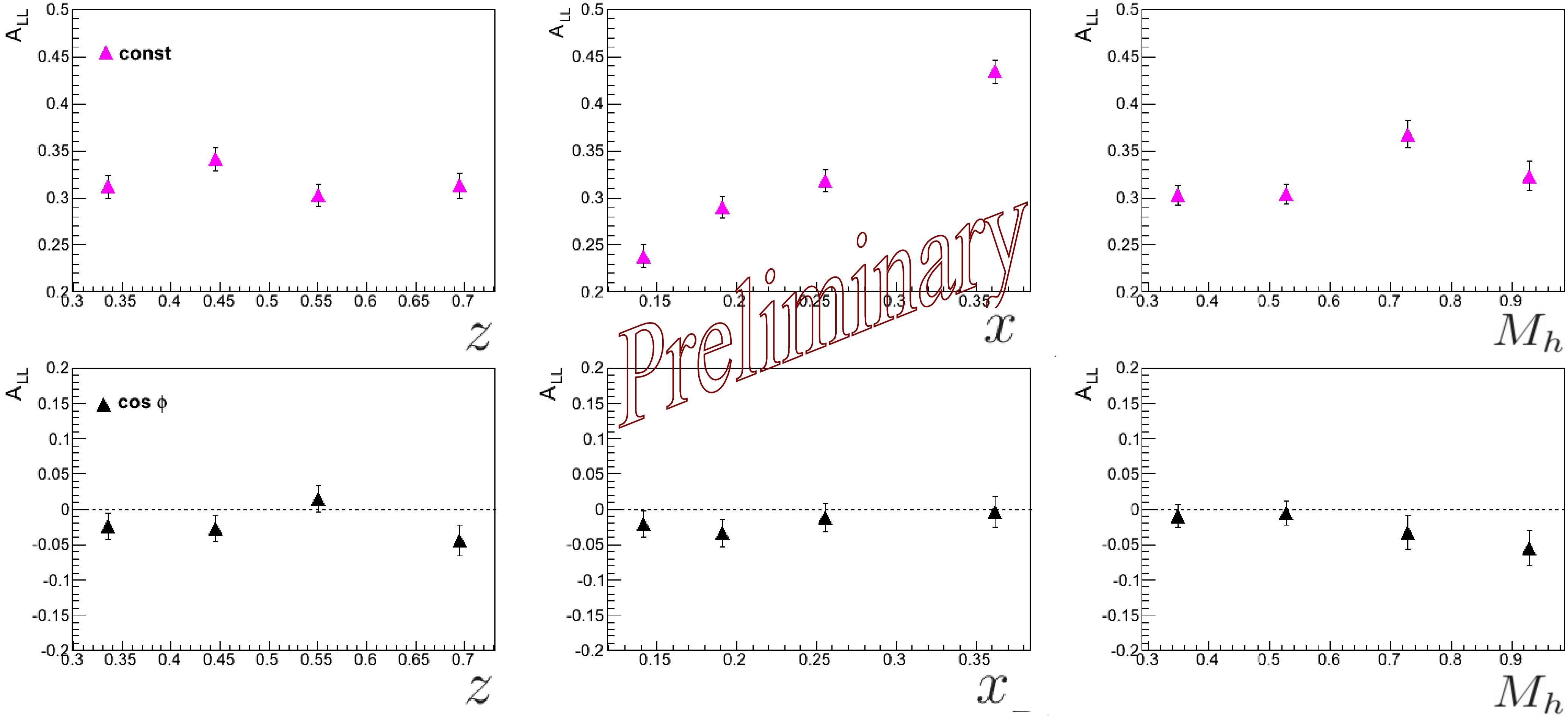

- Significantly non-zero A_{LL}^{const} asymmetries
- DF = 0.18 has been used

$$A_{LL}^{const} \propto g_1(x) D_1^q(z, \cos\theta, M_h)$$

$$A_{LL}^{\cos\varphi_R} \propto g_1(x) \tilde{D}^{\sphericalangle q}(z, \cos\theta, M_h)$$

Extracting A_1 from dihadron A_{LL}^{const} as a sanity check

- A_1 can be calculated as

$$A_1 \approx \frac{g_1 - \gamma^2 g_2}{f_1}$$

- In this check, A_1 was calculated assuming

$$g_2 = 0$$

- We measure $A_{LL}^{const} \approx \frac{F_{UU}}{F_{LL}}$

$$\approx \frac{g_1^q(x) D_1^q(z, \cos\theta, M_h)}{f_1^q(x) D_1^q(z, \cos\theta, M_h)}$$

Extracting A_1 from dihadron A_{LL}^{const} as a sanity check

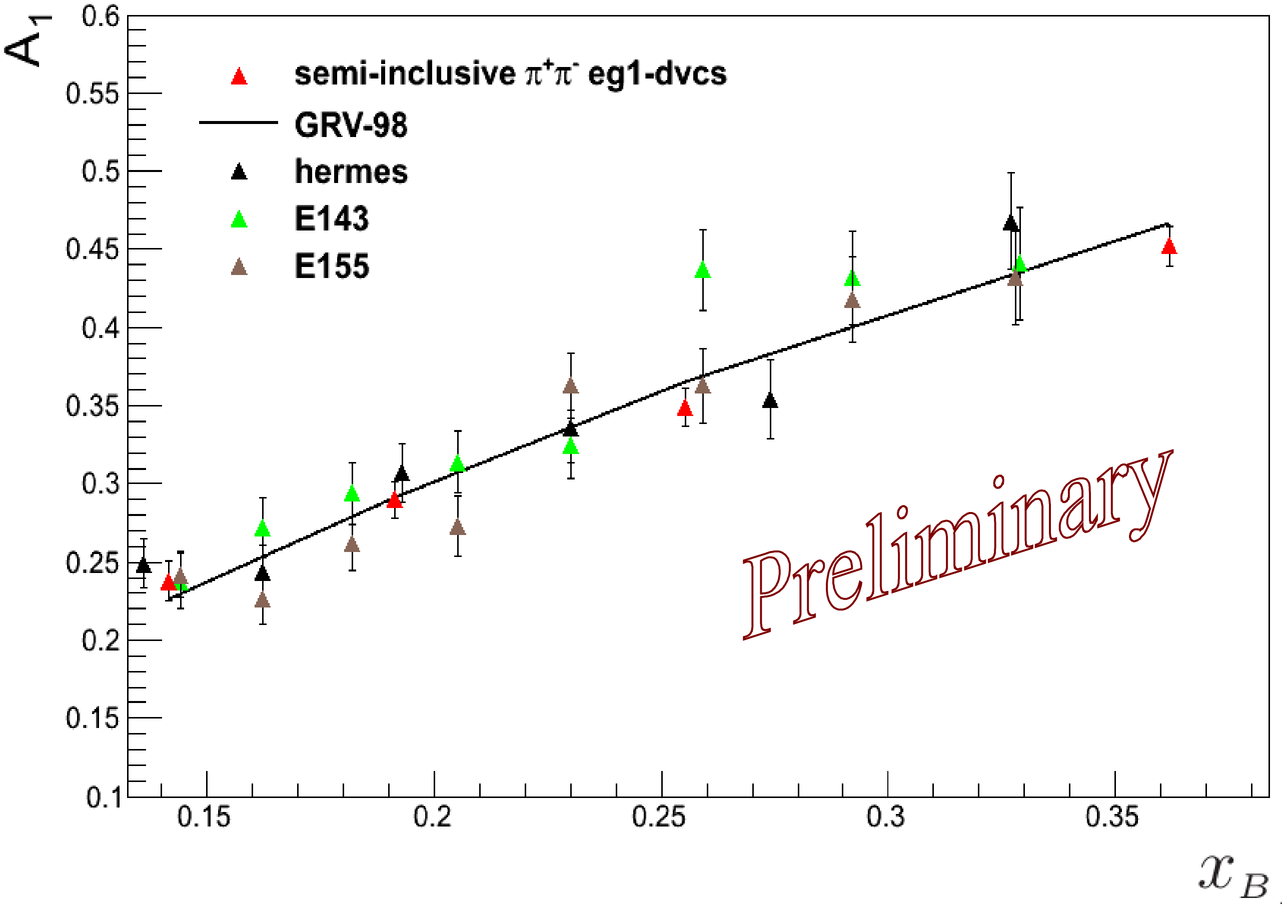

- A_1 can be calculated as

$$A_1 \approx \frac{g_1 - \gamma^2 g_2}{f_1}$$

- In this check, A_1 was calculated assuming

$$g_2 = 0$$

- We measure $A_{LL}^{const} \approx \frac{F_{UU}}{F_{LL}}$

$$\approx \frac{g_1^q(x) D_1^q(z, \cos\theta, M_h)}{f_1^q(x) D_1^q(z, \cos\theta, M_h)}$$

- This comparison shows that the present A_{LL}^{const} results are very consistent

Summary and Outlook

- dihadron SIDIS is a very powerful channel in order to access information about the collinear structure of the proton;
- CLAS detector at Jefferson Lab is an ideal place to provide such data;
- these are the first simultaneous measurements of the dihadron A_{LU} , A_{UL} and A_{LL} asymmetries;
- preliminary results of a non-zero BSA, TSA and DSA for $\pi^{+}\pi^{-}$ pairs have been shown;
- in the case of A_{LU} on both unpolarized H_2 and longitudinally-polarized NH_3 target indicates the absence of nuclear effects;

Outlook

- plan to look at $\pi^{+}\pi^{0}$ as well;